

# Stochastic Acceleration Model of Gamma-Ray Burst with Decaying Turbulence

Katsuaki Asano<sup>\*</sup> and Toshio Terasawa

*Institute for Cosmic Ray Research, The University of Tokyo, 5-1-5 Kashiwanoha, Kashiwa, Chiba 277-8582, Japan*

Accepted XXX. Received YYY; in original form ZZZ

## ABSTRACT

The spectral shape of the prompt emissions of gamma-ray bursts (GRBs) is typically expressed by the Band function: smooth joining of two power-law functions for high-energy and low-energy regions. To reveal the origin of the Band function, we revisit the stochastic acceleration model, in which electrons are accelerated via scattering with turbulent waves in the GRB outflow. The balance between the acceleration and synchrotron cooling yields a narrow energy-distribution similar to the Maxwellian distribution. The synchrotron spectrum becomes consistent with the observed hard photon index for the low-energy region. On the other hand, the narrow electron energy distribution contradicts the power-law spectrum for the high-energy region. We consider an evolution of the electron energy distribution to solve this problem. The turbulence and magnetic field induced by a certain hydrodynamical instability gradually decay. According to this evolution, the typical synchrotron photon energy also decreases with time. The time-integrated spectrum forms the power-law shape for the high-energy region. We discuss the required evolutions of the turbulence and magnetic field to produce a typical Band function. Although the decay of the turbulence is highly uncertain, recent numerical simulations for decaying turbulence seem comparatively positive for the stochastic acceleration model. Another condition required to reconcile observations is a much shorter duration of the stochastic acceleration than the dynamical timescale.

**Key words:** acceleration of particles – gamma-ray burst: general – radiation mechanisms: non-thermal – turbulence

## 1 INTRODUCTION

Gamma-ray bursts (GRBs) release isotropically equivalent energy of  $E_{\text{iso}} = 10^{51}\text{--}10^{54}$  erg as gamma-rays within a timescale of 0.1–100 s. The gamma-rays are considered to be emitted from relativistic jets with bulk Lorentz factor  $\Gamma > 100$ . The photon spectra are expressed with the conventional Band function (Band et al. 1993) with the parameters of the spectral peak energy  $\varepsilon_p$  (typically 100 keV–1 MeV), low-energy photon index  $\alpha$  ( $\sim -1$ ), and high-energy photon index  $\beta$  (roughly between  $-2$  and  $-3$ ). The short variability (1 ms–1 s) of GRB pulses is attributed to intermittent ejections of multiple emission regions from the central engine. In the classical internal shock model, this emission regions are shocked shells, where electrons are accelerated via the first-order Fermi acceleration (Fermi-I). However, the observationally typical low-energy index contradicts this scenario. Synchrotron emission from electrons injected via the Fermi-I process yields  $\alpha = -1.5$ , because the strong synchrotron cooling leads to an electron energy distribution of  $N(E_e) \propto E_e^{-2}$ .

Alternative ideas to resolve the low-energy photon index problem are photosphere models (Mészáros & Rees 2000; Giannios 2006; Pe’er et al. 2006; Asano & Mészáros 2013, and references therein), the Klein-Nishina effect on synchrotron self-Compton (SSC) process (Derishev et al. 2001; Bošnjak et al. 2009; Nakar et al. 2009; Wang et al. 2009; Bošnjak & Daigne 2014, and references therein), sudden damping of magnetic fields (Pe’er & Zhang 2006; Zhao et al. 2014), and inverse Compton models (Ghisellini & Celotti 1999; Stern & Poutanen 2004; Vurm & Poutanen 2009). In this paper, we revisit the second

<sup>\*</sup> E-mail: asanok@icrr.u-tokyo.ac.jp

order Fermi acceleration (Fermi-II) model of [Asano & Terasawa \(2009\)](#) (see also [Murase et al. 2012](#)). The Fermi-II process continuously accelerates electrons during the photon emission period. In this process, the resultant electron spectral index becomes harder than  $-2$  (e.g. [Schlickeiser 1984](#); [Park & Petrosian 1995](#); [Becker, Le & Dermer 2006](#); [Stawarz & Petrosian 2008](#); [Lefa, Rieger & Aharonian 2011](#)). As shown in [Asano & Terasawa \(2009\)](#), the acceleration timescale required to balance with the synchrotron cooling is much longer than the shock acceleration timescale with the Bohm limit; in other words, the electron mean free path in the Fermi-II models is much longer than the Larmor radius  $r_L$ . The scattering efficiency required in the Fermi-II models is not so high compared to the Fermi-I acceleration. [Asano & Terasawa \(2009\)](#) showed that the Fermi-II model naturally reproduces the low-energy photon index of the GRB spectrum. The required turbulence to accelerate electrons may be induced via the Kelvin–Helmholtz instability in the shear flow (e.g. [Zhang, Woosley & MacFadyen 2003](#); [Mizuta & Aloy 2009](#)) or at the boundary between the jet and cocoon ([Mészáros & Rees 2001](#); [Ramirez-Ruiz, Celotti & Rees 2002](#)). As radial modes, the Rayleigh–Taylor and Richtmyer–Meshkov instabilities are possible candidates to induce turbulence ([Matsumoto & Masada 2013](#)). In internal shock simulations with density fluctuation, the Richtmyer–Meshkov instability is excited ([Inoue et al. 2011](#)).

Interestingly, recent studies with the Fermi-II process also agrees with broadband blazar spectra ([Asano et al. 2014](#); [Diltz & Böttcher 2014](#); [Kakuwa et al. 2015](#); [Asano & Hayashida 2015](#)). The models reasonably reproduce very hard spectra seen in 1ES 0229+200 and 3C 279, and curved spectra for Mrk 421 and Mrk 501. Such results encourage us considering the Fermi-II process in GRB jets as well.

While numerical simulations of the Fermi-II were done in [Asano & Terasawa \(2009\)](#) and [Murase et al. \(2012\)](#), we analytically discuss the stochastic acceleration and emission in this paper. Whereas a simple Fermi-II model can easily produce observationally typical value of  $\alpha \sim -1$ , we mainly focus on the high-energy slope of the photon spectrum. The simplest Fermi-II model implies a Maxwellian-like narrow energy distribution for electrons, which contradicts the power-law photon spectrum above  $\varepsilon_p$ . To resolve this problem, we consider temporal evolutions of the electron energy distribution, which may be regulated by the evolutions of the turbulence, mean magnetic field, and electron injection process. The resultant evolution of the photon peak energy would produce a power-law envelope curve in the photon spectrum. Our purpose in this paper is to find ideal evolutions of the model parameters to reproduce the GRB photon spectrum. Although the lack of knowledge with the turbulence property and evolution in GRB jets prevents the final confirmation of the obtained results, our study will be an important step to probe the possibility of the Fermi-II process in GRB.

## 2 STOCHASTIC ACCELERATION AND COOLING

Gamma-rays are emitted from a collimated outflow relativistically moving toward observers. Hereafter, we discuss the electron acceleration and photon emission in the plasma rest frame. The values in the following equations are defined in the rest frame except for photon energy;  $\varepsilon'$  in the rest frame and  $\varepsilon = \Gamma\varepsilon'$  in the observer frame. We start from the same Fokker-Planck equation in [Asano & Terasawa \(2009\)](#) as

$$\frac{\partial N}{\partial t} = \frac{\partial}{\partial E_e} D_{EE} \frac{\partial N}{\partial E_e} - \frac{\partial}{\partial E_e} \left[ \left( 2 \frac{D_{EE}}{E_e} - \dot{E}_{\text{cool}} \right) N \right], \quad (1)$$

for the energy distribution of ultrarelativistic electrons  $N(E_e)$  in a certain volume. The energy diffusion coefficient  $D_{EE}$  is phenomenologically assumed to have a power-law form

$$D_{EE} = K_0 E_e^q. \quad (2)$$

For simplicity, we consider only synchrotron radiation for the cooling processes for electrons. The energy loss rate for an electron of  $E_e = \gamma_e m_e c^2$  is expressed as

$$\dot{E}_{\text{cool}}(\gamma_e) = \frac{4}{3} \sigma_T c \gamma_e^2 U_B, \quad (3)$$

where  $\sigma_T$  is the Thomson cross section, and  $U_B \equiv B^2/8\pi$  is the energy density of the magnetic field. The cooling time

$$t_c(\gamma_e) = \frac{6\pi m_e c}{\sigma_T B^2 \gamma_e}, \quad (4)$$

for gamma-ray emitting electrons is much shorter than the dynamical timescale (see e.g. [Asano & Terasawa 2009](#)). Therefore, when the synchrotron cooling balances with the stochastic acceleration, the electron energy distribution can be approximated by the steady solution for eq. (1) with a pile-up feature ([Schlickeiser 1984, 1985](#); [Aharonian, Atoyan & Nahapetian 1986](#); [Stawarz & Petrosian 2008](#); [Lefa, Rieger & Aharonian 2011](#)) as

$$N(E_e) = \frac{3N_{\text{tot}}}{\Gamma \left( \frac{6-q}{3-q} \right) E_0} \left( \frac{E_e}{E_0} \right)^2 \exp \left[ - \left( \frac{E_e}{E_0} \right)^{3-q} \right], \quad (5)$$

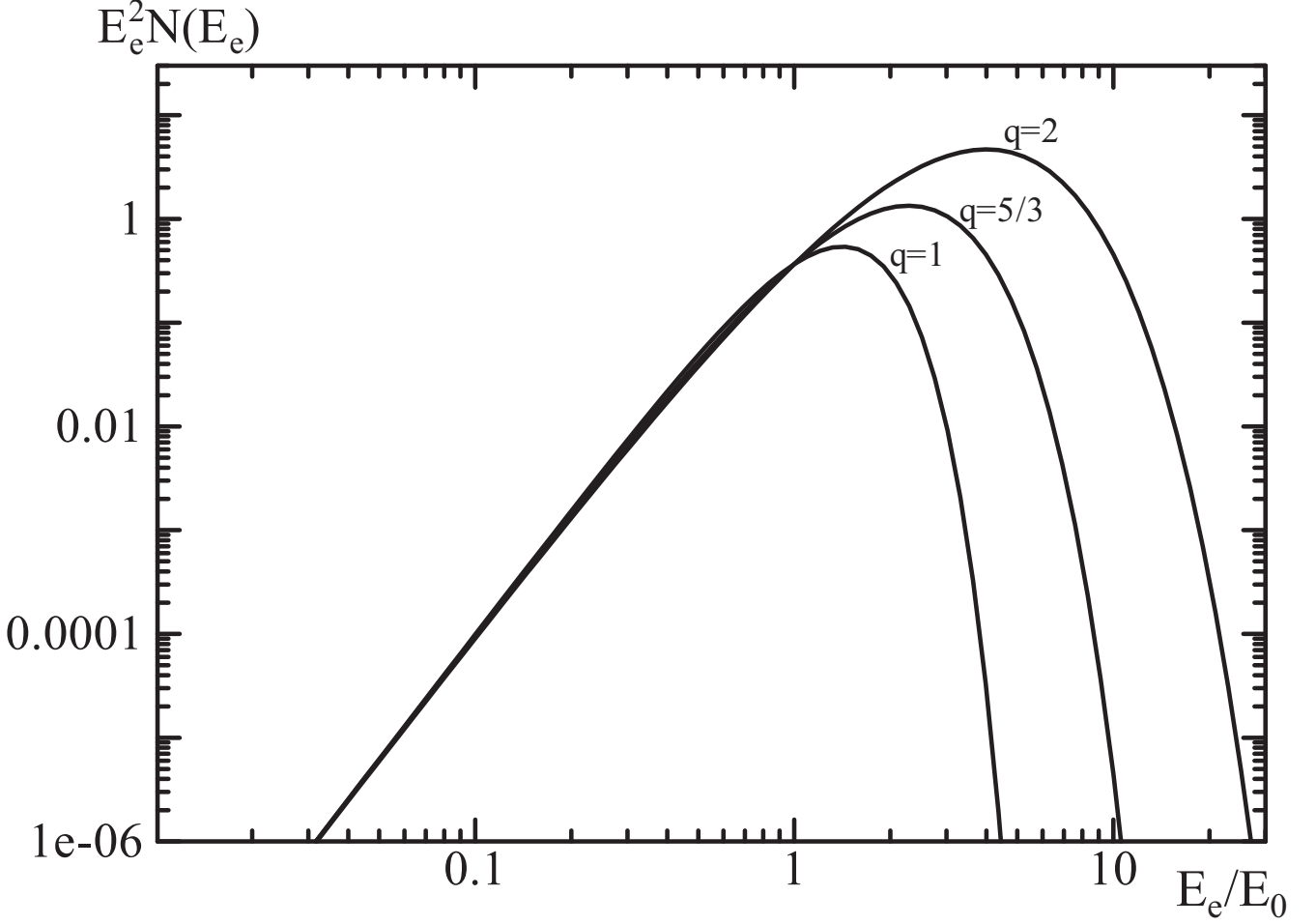


Figure 1. Steady solutions of electron energy distributions  $N(E_e)$  for various  $q$ .

where  $N_{\text{tot}}$  is the total electron number,  $\Gamma$  is the gamma function, and the cut-off energy is written as

$$E_0 = \left( \frac{6\pi(3-q)K_0 m_e^2 c^3}{\sigma_T B^2} \right)^{1/(3-q)}. \quad (6)$$

As shown in Figure 1, the spectral peak energy in  $E_e^2 N(E_e)$ -plot is sensitive to the index  $q$ .

Adopting the synchrotron function  $\mathcal{F}_{\text{syn}}(\chi) \equiv \chi \int_{\chi}^{\infty} d\xi K_{5/3}(\xi)$ , where  $K_{5/3}(\xi)$  is the modified Bessel function of the second kind (Rybicki and Lightman 1979), the photon production rate can be written as

$$\dot{N}_{\gamma}(\varepsilon') = \frac{\sqrt{3}e^3 B}{8\hbar m_e c^2 \varepsilon'} \int dE_e N(E_e) \mathcal{F}_{\text{syn}}\left(\frac{\varepsilon'}{\varepsilon'_{\text{typ}}}\right), \quad (7)$$

where the typical photon energy for electrons of  $E_e$  is

$$\varepsilon'_{\text{typ}}(E_e) = \frac{3\pi\hbar e B}{8m_e c} \gamma_e^2. \quad (8)$$

Substituting eq. (5) into equation (7),

$$\dot{N}_{\gamma}(\varepsilon') = \frac{\sqrt{3}e^2 m_e^2 c^3 N_{\text{tot}}}{\pi\Gamma\left(\frac{6-q}{3-q}\right) \hbar^2 E_0^3} \int dE_e \exp\left[-\left(\frac{E_e}{E_0}\right)^{3-q}\right] \int_{\varepsilon'/\varepsilon'_{\text{typ}}}^{\infty} d\xi K_{5/3}(\xi). \quad (9)$$

Defining  $x \equiv E_e/E_0$  and  $\varepsilon'_0 \equiv \varepsilon'_{\text{typ}}(E_0)$ ,

$$\dot{N}_{\gamma}(\varepsilon') = \frac{\sqrt{3}e^2 m_e^2 c^3 N_{\text{tot}}}{\pi\Gamma\left(\frac{6-q}{3-q}\right) \hbar^2 E_0^2} \int dx \exp(-x^{3-q}) \int_{x^{-2}\varepsilon'/\varepsilon'_0}^{\infty} d\xi K_{5/3}(\xi) \quad (10)$$

$$\equiv \frac{\sqrt{3}e^2 m_e^2 c^3 N_{\text{tot}}}{\pi\Gamma\left(\frac{6-q}{3-q}\right) \hbar^2 E_0^2} F_q\left(\frac{\varepsilon'}{\varepsilon'_0}\right). \quad (11)$$

Then, the spectral shape of the photon production rate is expressed by the non-dimensional function  $F_q(\varepsilon/\varepsilon_0)$ , which is

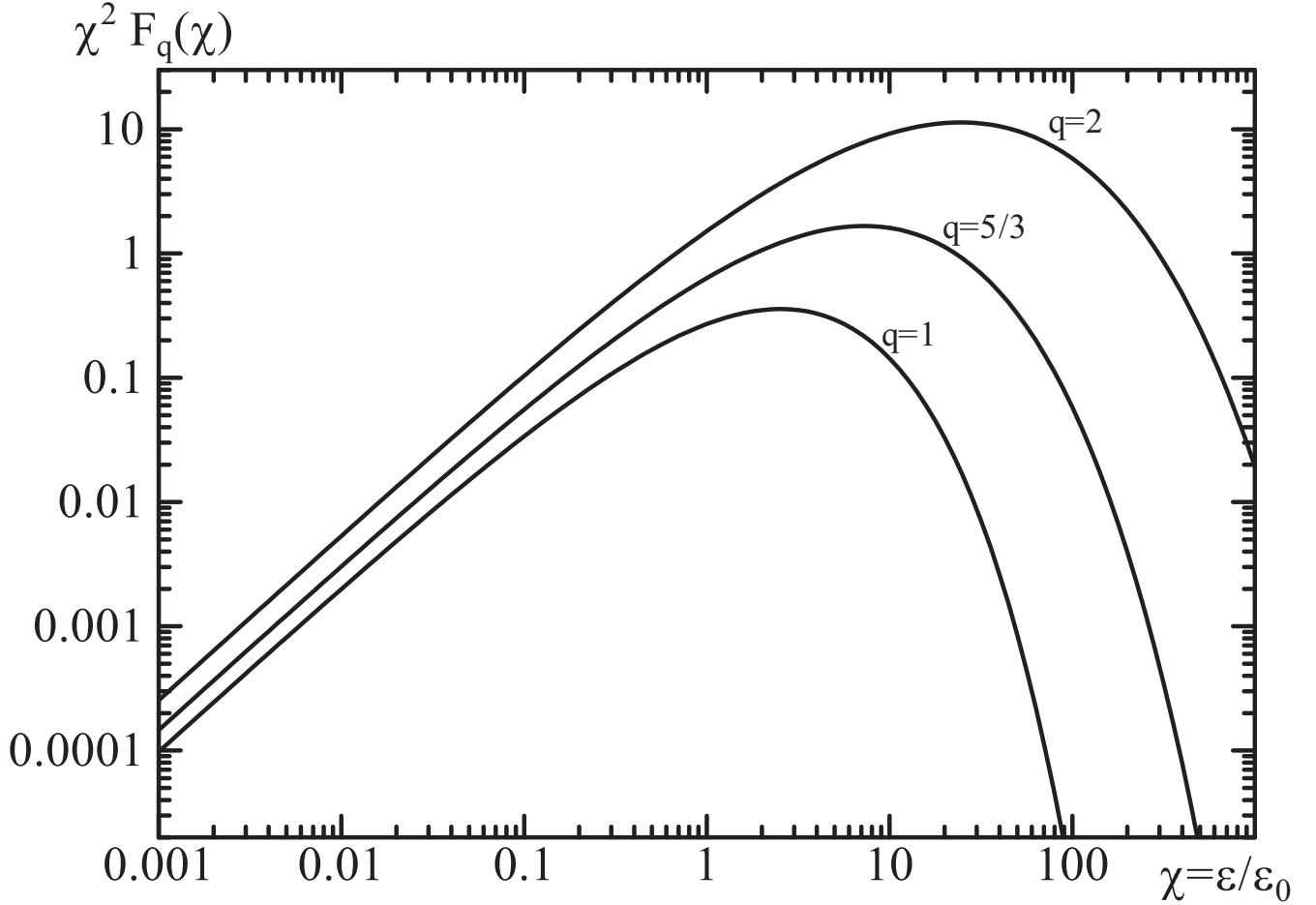


**Figure 2.** The non-dimensional functions  $F_q$  that provide the spectral shape of the photon production rate  $\dot{N}_\gamma$ .

**Table 1.**  $X_q \equiv \varepsilon_p/\varepsilon_0$ , the non-dimensional function  $I_q(0,0)$  is defined by eq. (24).

$q$	1	3/2	5/3	2
$X_q$	2.5	5.0	7.2	25
$I_q(0,0)$	1.1	3.0	5.3	35

obtained by integrating the function over  $x$  and  $\xi$ . In Figure 2, we show the functional shape of  $F_q$  for various  $q$ . The horizontal axis is normalized by  $\varepsilon_0$ . As shown in Figure 2, the spectral peaks in  $\varepsilon^2 \dot{N}_\gamma(\varepsilon)$ -plot are larger than  $\varepsilon_0$  (Fritz 1989; Zirakashvili & Aharonian 2007; Lefa, Rieger & Aharonian 2011). Here, we define this peak as  $\varepsilon_p \equiv X_q \varepsilon_0$ , and summarize values of  $X_q$  in Table 1.

We can choose fiducial parameters to agree with  $\varepsilon_p \sim 0.5$  MeV as

$$\varepsilon_p = 1.0 \left( \frac{\Gamma}{500} \right) \left( \frac{K_0}{10^2 \text{ s}^{-1}} \right)^2 \left( \frac{B}{10^4 \text{ G}} \right)^{-3} \text{ MeV}, \quad \text{for } q = 2, \quad (12)$$

$$\varepsilon_p = 0.72 \left( \frac{\Gamma}{500} \right) \left( \frac{K_0}{10^2 \text{ GeV}^{1/3} \text{ s}^{-1}} \right)^{3/2} \left( \frac{B}{10^4 \text{ G}} \right)^{-2} \text{ MeV}, \quad \text{for } q = 5/3, \quad (13)$$

$$\varepsilon_p = 0.65 \left( \frac{\Gamma}{500} \right) \left( \frac{K_0}{10^2 \text{ GeV}^{1/2} \text{ s}^{-1}} \right)^{4/3} \left( \frac{B}{10^4 \text{ G}} \right)^{-5/3} \text{ MeV}, \quad \text{for } q = 3/2, \quad (14)$$

$$\varepsilon_p = 0.52 \left( \frac{\Gamma}{500} \right) \left( \frac{K_0}{10^2 \text{ GeV s}^{-1}} \right) \left( \frac{B}{10^4 \text{ G}} \right)^{-1} \text{ MeV}, \quad \text{for } q = 1. \quad (15)$$

Note that the typical electron energy to emit 0.1–1 MeV photons is  $\sim$  GeV in the source rest frame for  $\Gamma = 500$  and  $B = 10^4$  G. The acceleration timescale  $t_{\text{acc}} \propto E_e^{2-q}$  implied above ( $\sim 10^{-2}$  s for GeV electrons) is much longer than the gyration period  $2\pi E_e/(eBc) \sim 7 \times 10^{-8} (E_e/\text{GeV})(B/10^4 \text{ G})^{-1}$  s. The Fermi-II model implies that the energy gain per

one scattering is  $\Delta E_e/E_e \sim \beta_{\text{eff}}^2$ , where  $\beta_{\text{eff}}$  is the effective turbulence velocity normalized by  $c$ . The energy fraction of the turbulence to the bulk jet energy is  $\sim \beta_{\text{eff}}^2$ . Though the turbulence velocity may be slower than the sound velocity in the relativistic plasma ( $\beta_{\text{eff}}^2 < 1/3$ ), the high radiative efficiency (e.g. Zhang et al. 2007) may require  $\beta_{\text{eff}}^2 \sim 0.1$ . This situation is similar to the standard shock acceleration models, in which a mildly relativistic shock is presumed. In both the cases, the energy source of the non-thermal electrons is the energy of mildly relativistic protons. Here, we assume that the turbulence has a characteristic scale, namely typical eddy size  $l_{\text{edd}}$ . If the turbulence spectrum ranges in significantly short wavelengths comparable to the Larmor radius  $r_L \sim 300(E_e/10^9 \text{ eV})(B/10^4 \text{ G})^{-1}$ , the mean free path is written as  $l_{\text{mfp}} \sim r_L B^2/\delta B_{\text{eff}}^2$  (Blandford & Eichler 1987). Inside the eddies  $\beta_{\text{eff}}^2 \ll 0.1$ , while only electrons moving across eddies are scattered via nonresonant mirror interaction (transit time damping) arising from compressible (acoustic) modes (Ptuskin 1988; Cho & Lazarian 2006; Yan & Lazarian 2008; Lynn et al. 2014) with  $\beta_{\text{eff}}^2 \sim 0.1$ . When the diffusion time  $l_{\text{edd}}^2/(cl_{\text{mfp}})$  is much longer than the eddy timescale  $t_{\text{edd}} = l_{\text{edd}}/(c\beta_{\text{eff}})$ , the timescale  $t_{\text{acc}}\beta_{\text{eff}}^2$  may correspond to the eddy timescale so that  $l_{\text{edd}} \sim ct_{\text{acc}}\beta_{\text{eff}}^3 \sim 10^7(t_{\text{acc}}/10^{-2} \text{ s})(\beta_{\text{eff}}^2/0.1)^{3/2} \text{ cm}$ . Finally we obtain  $D_{EE} \sim \beta_{\text{eff}}^2 E_e^2/t_{\text{edd}} \propto \beta_{\text{eff}}^3/l_{\text{edd}}$ .

However, there may be a transition scale at the wavelength where the kinetic energy is comparable to the magnetic energy. At the shorter wavelength than the transition scale, the power-spectrum of the turbulence is steeply damped. Then, the mean free path of electrons may be elongated as long as the eddy scale. In this case, we obtain  $l_{\text{edd}} \sim ct_{\text{acc}}\beta_{\text{eff}}^2 \sim 3 \times 10^7(t_{\text{acc}}/10^{-2} \text{ s})(\beta_{\text{eff}}^2/0.1) \text{ cm}$  and  $D_{EE} \propto \beta_{\text{eff}}^2/l_{\text{edd}}$ .

The above qualitative discussion is still insufficient to conclude the acceleration property in the turbulence. In the following discussion we maintain the phenomenological parameterization for the energy diffusion coefficient with arbitrary  $q$  and  $K_0$ .

### 3 DECAYING TURBULENCE

If the parameters in equation (11), such as  $\varepsilon_0$  etc., remain constant during the emission period, the photon spectrum for observers is just a blue-shifted spectrum of  $\dot{N}_\gamma(\varepsilon')$ . As shown in Figure 2, the spectral shape with a sharp cut-off may contradict the observed Band spectra especially for smaller  $q$ . However, the efficiency of the stochastic acceleration is expected to decay with time. Then, the typical photon energy  $\varepsilon_0$  would shift to lower energy. Such an evolution of the photon emission spectrum can produce a high-energy power-law part in the time-integrated spectrum.

Since the time-integrated photon spectrum is written as

$$N_\gamma(\varepsilon') = \int dt \dot{N}_\gamma(\varepsilon') \quad (16)$$

$$= \frac{\sqrt{3}e^2 m_e^2 c^3}{\pi \Gamma\left(\frac{6-q}{3-q}\right) \hbar^2} \int dt \frac{N_{\text{tot}}}{E_0^2} F_q\left(\frac{\varepsilon'}{\varepsilon_0}\right), \quad (17)$$

the temporal evolutions of the two quantities,  $\varepsilon_0$  and  $N_{\text{tot}}/E_0^2$ , determine the final photon spectral shape. Let us assume that all the parameters evolve following power-laws of  $(t + t_{\text{tbl}})$  and the turbulence suddenly disappears at  $t = t_f$  for simplicity. The duration  $t_f$  is defined as the energy transfer timescale from the turbulence to electrons. The parameter  $t_{\text{tbl}}$ , which may correspond to the production timescale of the turbulence, is introduced to avoid divergence at  $t = 0$ . Hereafter, the combinations of the parameters are assumed to behave as  $N_{\text{tot}}/E_0^2 \propto (t + t_{\text{tbl}})^a$  and  $\varepsilon'_0 \propto BE_0^2 \propto (t + t_{\text{tbl}})^{-b}$  with indices  $a$  and  $b$ . Here we explore ideal pairs of the phenomenological indices  $a$  and  $b$  to reproduce typical GRB spectra.

As will be discussed below, the index  $a$  may be  $\lesssim 2$ . In Figure 3, we plot the photon spectrum  $N_\gamma(\varepsilon)$  with  $q = 5/3$ ,  $a = 2$ , and  $t_f = 100t_{\text{tbl}}$  for various  $b$ . The photon energy is normalized by  $\varepsilon_{0,i}$ , which is  $\varepsilon_0$  at  $t = 0$ . As  $b$  becomes large, the faster decay of  $\varepsilon_0$  makes a lower spectral peak energy. Since  $\int dt \dot{N}_\gamma(\varepsilon'_0) \propto (t + t_{\text{tbl}})^{1+a}$ , the photon index parameter in the Band spectrum would be approximated as

$$\beta = -\frac{1+a}{b}. \quad (18)$$

Therefore, as shown in Figure 3, the parameter values of  $b$  between 1 and 1.5 are favorable for  $a = 2$  to adjust the index between  $-2$  and  $-3$ . This result is common irrespective of the value of  $q$ ; the spectral shapes for other  $q$  are similar to each other. Especially, the case of  $b = 1$  in Figure 3 is well fitted with the typical Band parameters ( $\alpha = -1$  and  $\beta = -2.5$ ) below  $10\varepsilon_p$ . The obtained Band parameter  $\varepsilon_p$  is slightly larger than the final value of  $X_q \varepsilon_0 = 7.2(t + t_{\text{tbl}})^{-1} \varepsilon_{0,i} \simeq 0.07\varepsilon_{0,i}$ , but the difference may be hard to be seen as shown in the figure. The spectral curvature around  $\varepsilon_p$  leads to the difference between the Band parameter  $\beta = -2.5$  below  $10\varepsilon_p$  and the asymptotic value  $-(1+a)/b = -3$ . Note that, however, in most cases the photon statistics above  $10\varepsilon_p$  (typically a few MeV) is insufficient to detect the spectral break or curvature.

Here we attempt to associate the phenomenological parameters  $a$  and  $b$  with the evolutions of the turbulence and electron injection. Initially the diffusion coefficient and magnetic field are larger than the values assumed in eqs. (12)–(15). Then, the acceleration timescale is gradually elongated, and settles down to the value suited for  $\varepsilon_p \sim 0.5 \text{ MeV}$  at  $t = t_f$ . Let us write  $K_0 \propto t^{-s}$  and  $B \propto t^{-w}$ ,  $E_0 \propto t^{(2w-s)/(3-q)}$ . Then,  $\varepsilon'_0 \propto BE_0^2 \propto t^{-w+2(2w-s)/(3-q)}$ . The total number of electrons may

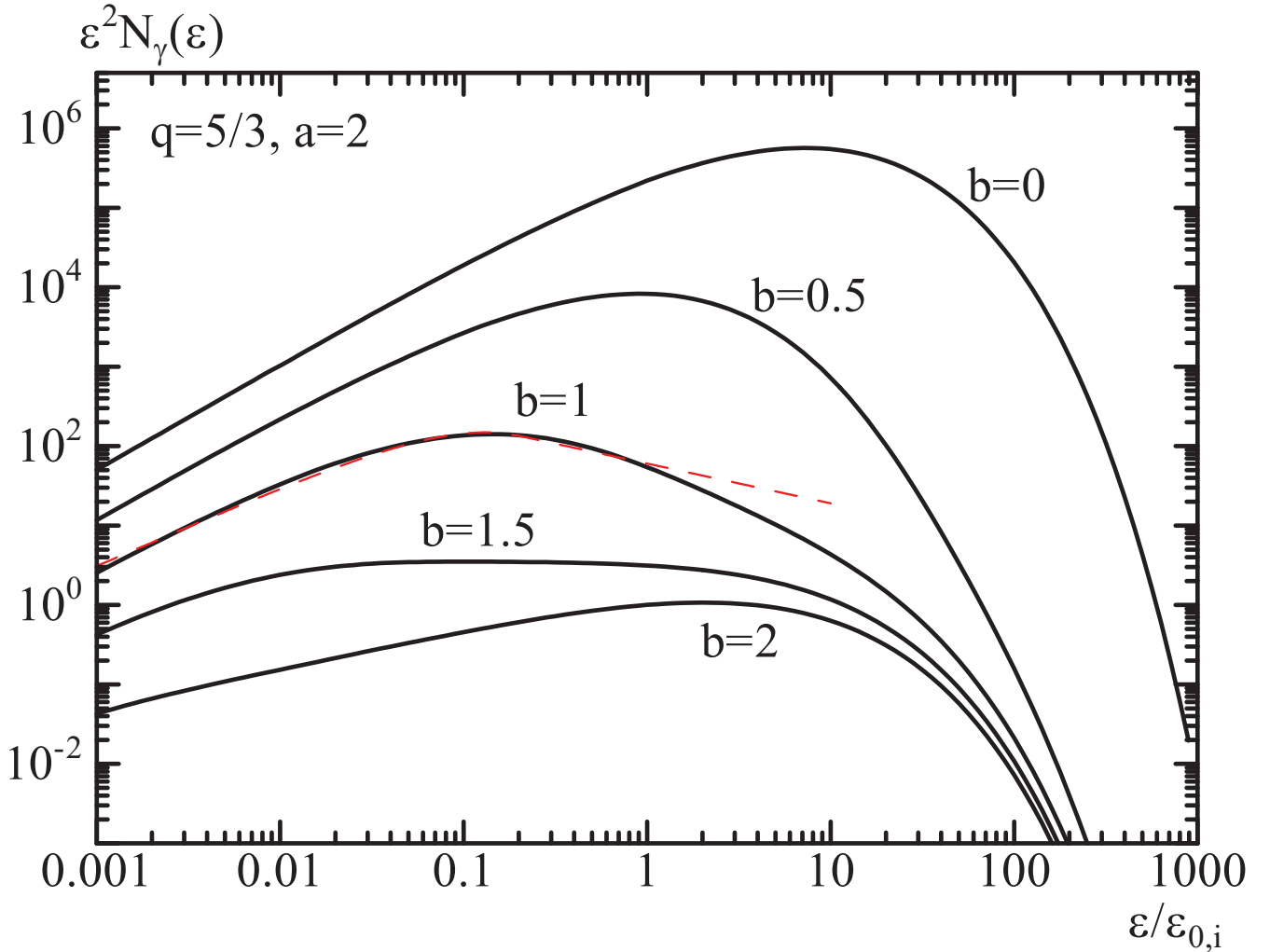


**Figure 3.** Photon spectrum with  $q = 5/3$ ,  $a = 2$ , and  $t_f = 100t_{\text{tbl}}$  for various  $b$ . The dashed line is the Band function with  $\alpha = -1$ ,  $\beta = -2.5$ , and  $\varepsilon_p = 0.13\varepsilon_{0,i}$ .

increase following the injection rate<sup>1</sup>. If we express this as  $N_{\text{tot}} \propto t^n$ ,  $t\dot{N}_\gamma(\varepsilon'_0) \propto tN_{\text{tot}}E_0^{-2} \propto t^{1+n-2(2w-s)/(3-q)}$ . As a result, the parameters  $a$  and  $b$  are written with the indices defined above ( $s$ ,  $w$ , and  $n$ ) as

$$a = n - 2\frac{2w-s}{3-q}, \quad b = w - 2\frac{2w-s}{3-q}. \quad (19)$$

Although the parameters  $s$ ,  $w$ , and  $n$  are highly uncertain, some discussion of the interaction between the turbulence and electrons may provide insight into the required condition,  $(1+a)/b = 2-3$ , in our Fermi-II model. The average energy gain of electrons per one scattering by waves is proportional to  $\beta_{\text{eff}}^2 \sim \max(\beta_{\text{W}}^2, \beta_{\text{A}}^2)$ , where  $\beta_{\text{W}}$  and  $\beta_{\text{A}}$  are the turbulence velocity and Alfvén velocity normalized by  $c$ , respectively. In our case, the required electron energy density is higher than the magnetic field density so that  $\beta_{\text{W}}^2 > \beta_{\text{A}}^2$  is likely. In the simulations of [Inoue et al. \(2011\)](#), when a relativistic shock propagates inhomogeneous medium, the Richtmyer–Meshkov instability is excited and the turbulence starts to decay after a few eddy-turnover times. If we adopt those results,  $\beta_{\text{W}}^2 \propto U_{\text{K}} \propto t^{-1.3}$  and  $\delta B^2 \propto U_B \propto t^{-0.7}$ . As we discussed in the last part of §2, the diffusion coefficient may behave as  $D_{EE} \propto \beta_{\text{W}}^3/l_{\text{edd}}$  (short-mfp model) or  $\beta_{\text{W}}^2/l_{\text{edd}}$  (long-mfp model). The long-mfp model with a constant  $l_{\text{edd}}$  and the simulation result of [Inoue et al. \(2011\)](#) lead to  $q = 2$ ,  $s = 1.3$ . Since the average field  $B \propto \delta B$  in this highly turbulent plasma, we obtain  $w = 0.35$ . The above values imply  $b = 1.55$  and  $a = n + 1.2$ . Therefore, the constant injection rate  $n = 1$  seems favorable, while the short-mfp model requires an ad hoc value of  $n \sim 3$ .

Other recent MHD simulations ([Zrake 2014](#); [Brandenburg, Kahnishvili & Tevzadze 2015](#)) show inverse transfers from small to large turbulence-scales in spite of the absence of magnetic helicity. In such cases, the evolutions of the turbulence scale and energy densities depend on their initial conditions ([Olesen 1997](#)). In the relativistic simulation in [Zrake \(2014\)](#), the longest

<sup>1</sup> Note that the electron number was assumed to be constant in the simulations of [Asano & Terasawa \(2009\)](#)

wavelength evolves as  $k_M \propto t^{-2/5}$  and  $U_B \propto t^{-14/15}$ , while the non-relativistic simulation of [Brandenburg, Kahnishvili & Tevzadze \(2015\)](#) shows  $k_M \propto t^{-1/2}$  and  $U_B \propto t^{-1}$ . The indices of the power-spectral density for  $k > k_M$  are 2 in both the two simulations. The simplest analytical discussion in [Son \(1999\)](#), considering the evolution of patchy turbulence, concludes  $k_M \propto t^{-2/5}$  and  $U_K \propto U_B \propto t^{-6/5}$ , which are not far from the simulation results. From the derived indices  $w = 3/5$  and  $s = 8/5$  for the long-mfp model, finally we obtain the phenomenological indices  $a = n + 4/5$  and  $b = 7/5$ . If the electron injection rate is constant ( $n = 1$ ), the photon index becomes an ideal value  $\beta = -(1 + a)/b = -2$ . This primitive model of the turbulence evolution also predicts a reasonable range of the photon index. The electron acceleration affects the decay of turbulence, which modifies the estimate of the photon index. More quantitative discussion based on numerical simulations is necessary to determine the value  $\beta$ . On the other hand, the short-mfp model requires  $n = 3$  again.

Although the above discussion does not always validate the Fermi-II model, we do not find any discouraging evidence so far. The next step is a study to verify the fundamental acceleration process in such turbulence, but this is beyond our scope in this paper.

We have neglected the effect of inverse Compton scattering. However, most of GRBs do not show the extra component that can be interpreted as the inverse Compton component ([Ackermann et al. 2012](#)). Even when the magnetic field is weak compared to the electron energy density, the lack of the inverse Compton component can be explained by the Klein-Nishina effect (e.g. [Asano & Mészáros 2011](#)). The numerical simulations of [Asano & Terasawa \(2009\)](#) also shows that the inverse Compton emission does not greatly affect the synchrotron spectrum.

#### 4 SECONDARY ELECTRON-POSITRON PAIRS

The continuous electron acceleration increases the gamma-ray energy emitted from one electron so that the required electron number is less than the standard shock acceleration models, in which all electrons are assumed to be accelerated. In our model there should be a condition for electrons to enter the acceleration process. The injection mechanism is uncertain similarly to that in the shock acceleration. The electron injection mechanism may be sub-shocks ([Narayan & Kumar 2009](#)) or magnetic reconnection in the turbulence. At least, the electron should be relativistic to be in the acceleration process we have assumed. Hereafter, we assume the threshold energy of electrons/positrons,  $\gamma_{\text{th}} m_e c^2$ , to be accelerated by turbulence.

We have assumed a gradual increase of the electron number by a stable electron injection. However, high energy photons produce secondary electron-positron pairs via  $\gamma\gamma$ -absorption. Those pairs can be also accelerated by turbulence and emit high-energy photons. If such pairs dominate the lepton number, the non-linear growth of the electron/positron number occurs, which results in a sudden increase of pairs. Those non-linear evolution of the electron/positron number is not favorable to produce a Band-like spectrum. In this section, we estimate the contribution of the secondary pairs under the situation we have assumed.

First, we obtain the required number of electrons in the Fermi-II model. In our model, following the power-law evolution of  $(1 + t/t_{\text{tbl}})^{-b}$ , the typical photon energy decays from  $\varepsilon_{0,i}$  to  $\varepsilon_{0,f}$ . Denoting the values of  $N_{\text{tot}}$  and  $E_0$  at  $t = t_f$  as  $N_{\text{tot},f}$  and  $E_{0,f}$ , respectively, the total photon energy in the comoving frame is written as

$$E'_{\text{ph}} = \int d\varepsilon' \varepsilon' N_\gamma(\varepsilon') = \frac{\sqrt{3}e^2 m_e^2 c^3}{\pi \Gamma \left( \frac{6-q}{3-q} \right) \hbar^2} \frac{N_{\text{tot},f}}{E_{0,f}^2} \left( 1 + \frac{t_f}{t_{\text{tbl}}} \right)^{-a-1} t_f \varepsilon_{0,i}'^2 \times \int dy \int_0^{t_f/t_{\text{tbl}}} dx y (1+x)^a F_q \left( \frac{y}{(1+x)^{-b}} \right). \quad (20)$$

The peak energy for observers is written with the final value of  $\varepsilon_0$  as  $\varepsilon_p \simeq \Gamma X_q \varepsilon_{0,f}'$ . Then, we obtain

$$\Gamma \varepsilon_{0,i}' = \frac{\varepsilon_p}{X_q} \left( 1 + \frac{t_f}{t_{\text{tbl}}} \right)^b. \quad (21)$$

Substituting  $E_{0,f}/(m_e c^2)$  for  $\gamma_e$  in eq. (8), we obtain

$$\frac{\varepsilon_{0,i}'}{E_{0,f}^2} = \left( 1 + \frac{t_f}{t_{\text{tbl}}} \right)^b \frac{3\pi \hbar \varepsilon B_f}{8m_e c} \left( \frac{1}{m_e c^2} \right)^2, \quad (22)$$

as well, where  $B_f$  is the final value of  $B$ . Adopting those equations, the isotropically-equivalent total photon energy in one pulse is expressed as

$$E_{\text{ph}} = \Gamma \int d\varepsilon' \varepsilon' N_\gamma(\varepsilon') = \frac{3\sqrt{3}e^3}{8\Gamma \left( \frac{6-q}{3-q} \right) \hbar m_e c^2} N_{\text{tot},f} B_f t_f \frac{\varepsilon_p}{X_q} I_q(a, b), \quad (23)$$



where the non-dimensional function

$$I_q(a, b) \equiv \left(1 + \frac{t_f}{t_{\text{tbl}}}\right)^{2b-a-1} \int dy \int_0^{t_f/t_{\text{tbl}}} dx y (1+x)^a F_q \left(\frac{y}{(1+x)^{-b}}\right) \quad (24)$$

$$\simeq \frac{1}{1+a-2b} \int dy y F_q(y) = \frac{1}{1+a-2b} I_q(0, 0), \quad (25)$$

for  $1+a-2b > 0$ , and the final approximation has been obtained with  $t_f/t_{\text{tbl}} \gg 1$ . The values of  $I_q(0, 0)$  for various  $q$  are tabulated in Table 1.

While the observables are  $E_{\text{ph}}$  and  $\varepsilon_{\text{p}}$ , the model parameters to determine the total photon energy are  $N_{\text{tot},f}$ ,  $B_f$ , and  $t_f$ . The timescale  $t_f$  can be considered as the dissipation timescale of the turbulence into electrons. Alternatively, as will be explained below, the injection of secondary electron–positron pairs may control the duration  $t_f$ . The timescale  $t_f$  can be shorter than the dynamical timescale  $t_{\text{dyn}} \equiv R/(c\Gamma)$  as supposed in [Asano & Terasawa \(2009\)](#). Note  $t_{\text{dyn}} = \Gamma t_v = 50(\Gamma/500)(t_v/0.1 \text{ s})$  s, where  $t_v \equiv R/(c\Gamma^2)$  is the variability timescale for observers. But  $t_f$  may be longer than the cooling timescale

$$t_c(\varepsilon_{\text{p}}) \simeq \frac{6\pi}{\sigma_{\text{T}} B^{3/2}} \sqrt{\frac{\hbar \varepsilon \Gamma m_e c}{\varepsilon_{\text{p}}}} = 2.6 \left(\frac{\Gamma}{500}\right)^{1/2} \left(\frac{B_f}{10^4 \text{ G}}\right)^{-3/2} \left(\frac{\varepsilon_{\text{p}}}{0.5 \text{ MeV}}\right)^{-1/2} \text{ ms}. \quad (26)$$

The total photon energy is written as

$$E_{\text{ph}} \sim 1.9 \times 10^{51} \left(\frac{N_{\text{tot},f}}{10^{50}}\right) \left(\frac{t_f}{0.1 \text{ s}}\right) \left(\frac{B_f}{10^4 \text{ G}}\right) \left(\frac{\varepsilon_{\text{p}}}{0.5 \text{ MeV}}\right) \text{ erg}, \quad (27)$$

for  $q = 5/3$  with  $I_q(0, 0)$ . The required electron number  $N_{\text{tot},f}$  to achieve  $\sim 10^{51}$  erg is much less than the number in the classical shock acceleration model by a factor of  $\sim t_c/t_f$ . The assumed timescale above implies a significantly longer scale than the eddy scale estimated in §2 as  $ct_f \sim 100l_{\text{edd}}$ .

Let us estimate the number of the secondary pairs. We approximate the photon-density spectrum for  $\varepsilon' > \varepsilon'_{\text{p}}$  by a power-law

$$n_{\gamma}(\varepsilon') \simeq \frac{n_0}{\varepsilon_{\text{p}}} \left(\frac{\varepsilon'}{\varepsilon_{\text{p}}}\right)^{\beta}. \quad (28)$$

Although the result will be independent of the width of the emission region, here we assume the width as  $ct_f/3$ . Then, the normalization in eq. (28) becomes

$$n_0 \simeq \frac{-3(\beta+2)E_{\text{ph}}}{4\pi R^2 ct_f \varepsilon_{\text{p}}}. \quad (29)$$

In this case, the optical depth for  $\gamma\gamma$ -absorption is written as

$$\tau_{\gamma\gamma}(\varepsilon') \simeq 0.1\sigma_{\text{T}} n_0 \frac{ct_f}{3} \left(\frac{\varepsilon' \varepsilon'_{\text{p}}}{m_e^2 c^4}\right)^{-\beta-1}, \quad (30)$$

([Asano & Takahara 2003](#), and supporting material in [Abdo et al. 2009](#)). This results in

$$\tau_{\gamma\gamma}(\gamma m_e c^2) \simeq 0.1\sigma_{\text{T}} \frac{-(\beta+2)E_{\text{ph}}}{4\pi R^2 \varepsilon_{\text{p}}} \Gamma^{1+\beta} \left(\frac{\gamma \varepsilon_{\text{p}}}{m_e c^2}\right)^{-\beta-1}. \quad (31)$$

When  $\tau_{\gamma\gamma}(\gamma_{\text{th}} m_e c^2) \ll 1$ , the number of the secondary pairs above  $\gamma_{\text{th}} m_e c^2$  is independent of  $\gamma_{\text{th}}$  as

$$N_{\pm}(\gamma > \gamma_{\text{th}}) \sim \tau_{\gamma\gamma}(\gamma_{\text{th}} m_e c^2) 4\pi R^2 \frac{ct_f}{3} \gamma_{\text{th}} m_e c^2 n'_{\gamma}(\gamma_{\text{th}} m_e c^2) \quad (32)$$

$$= 0.1 \frac{(\beta+2)^2 \sigma_{\text{T}} m_e c^2 E_{\text{ph}}^2}{4\pi c^2 t_f^2 \varepsilon_{\text{p}}^3} \Gamma^{2\beta-2} \left(\frac{\varepsilon_{\text{p}}}{m_e c^2}\right)^{-2\beta-1}. \quad (33)$$

For  $\beta = -2.5$ , the number becomes

$$N_{\pm}(\gamma > \gamma_{\text{th}}) \sim 2.8 \times 10^{49} \left(\frac{t_v}{0.1 \text{ s}}\right)^{-2} \left(\frac{E_{\text{ph}}}{10^{51} \text{ erg}}\right)^2 \left(\frac{\Gamma}{500}\right)^{-7} \left(\frac{\varepsilon_{\text{p}}}{0.5 \text{ MeV}}\right), \quad (34)$$

which is smaller than the number  $N_{\text{tot},f}$  adopted in eq. (27), but of considerable quantity. If the condition  $N_{\pm} \ll N_{\text{tot},f}$  is critical for the model, we need to adjust the model parameters, e.g., increase of  $N_{\text{tot},f}$  by a smaller  $B_f t_f$  or decrease of  $N_{\pm}$  by a larger  $\Gamma$ . As shown in Figure 3, however, the photon spectrum may not be the extension of the single power-law as far as the energy of  $\Gamma \gamma_{\text{th}} m_e c^2 \sim 26(\Gamma/500)(\gamma_{\text{th}}/100)$  GeV. In such cases, the number of the pairs is smaller than the above estimate. The numerical simulations in [Asano & Terasawa \(2009\)](#) is a case where the contribution of the secondary pairs is negligible, while the pairs injected via the hadronic cascade dominates in the model of [Murase et al. \(2012\)](#).

Another possibility is that the sudden increase of electrons/positrons due to the non-linear effect triggers the damping of the turbulence. As long as the total energy in the turbulence is finite, an explosive increase of the lepton number causes a strong dissipation of the turbulence. In that case, the average energy of the electrons/positrons in the acceleration process also suddenly decreases. This leads to inefficiency of gamma-ray emission. Such a non-linear effect between the turbulence and secondary pairs may finally determine the duration  $t_f$ .



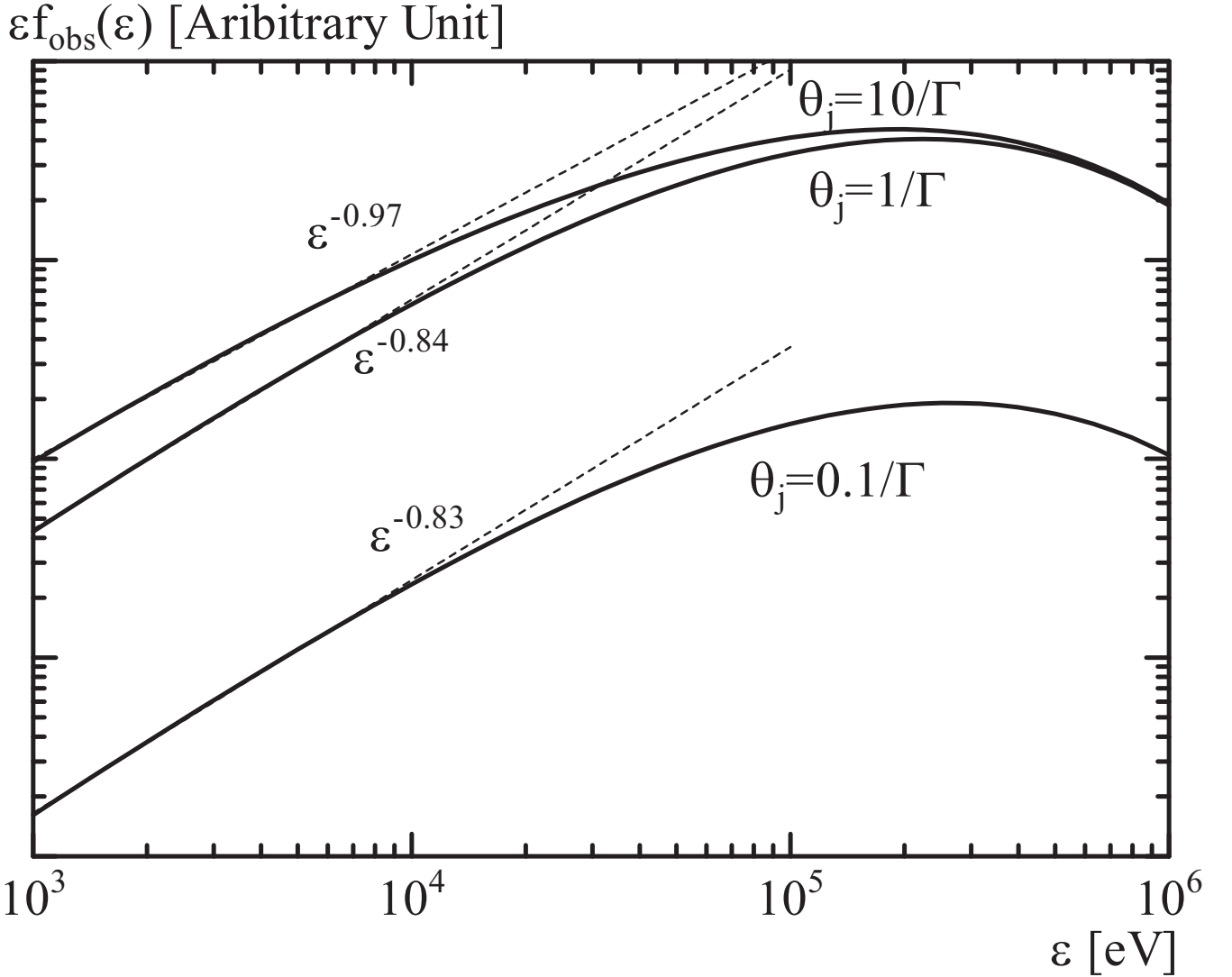


Figure 4. Observable photon spectra for various jet opening angles.

In conclusion, the turbulence decay timescale  $t_f$ , which depends on the electron injection rate including the secondary pairs, should be much shorter than the dynamical timescale in the stochastic acceleration model. Note that this timescale is still much longer than the presumed energy-transfer timescale from protons to electrons in the shock acceleration models.

## 5 OFF-AXIS CONTRIBUTION

In this section we switch a topic to focus on the low-energy portion of the Band spectrum. One may consider that the hard electron spectrum leads to the “synchrotron limit”  $\alpha = -2/3$  for the photon index. Such a hard spectral index is not frequently detected. However, the best model in Figure 3 ( $b = 1$ ) is well fitted with the typical Band parameter  $\alpha = -1$ . The difference between the model and Band function is hard to be recognized observationally. Moreover, the contribution of the off-axis emission can soften the photon spectrum for observers. The dominant contribution to photons detected by an observer is emitted from the jet surface within the opening angle (relative to the line-of-sight) of  $1/\Gamma$  because of the relativistic beaming. However, the emission from  $\theta > 1/\Gamma$  can modify the spectrum as shown in Figure 4.

Here, we have assumed that photons distributing isotropically in the rest frame are emitted from a sphere expanding with  $\Gamma = 300$ . The photon spectrum in the rest frame has the form of  $F_q$  with  $q = 5/3$ . We have numerically integrated photons emitted from the surface within  $\theta \leq \theta_j$  taking into account the relativistic beaming effects; photon energy  $\varepsilon' = \varepsilon\Gamma(1 - \beta_{\text{sh}} \cos \theta)$ , solid angle  $d\Omega = \Gamma^2(1 - \beta_{\text{sh}} \cos \theta)^2 d\Omega'$ , photon number  $dN = dN'$ , surface  $dS = dS'$ , angle  $\cos \theta' = (\cos \theta - \beta_{\text{sh}})/(1 - \beta_{\text{sh}} \cos \theta)$ , and  $dN'/(d\Omega' dS') \propto |\cos \theta'|$  (see Asano & Mészáros 2011), where  $\beta_{\text{sh}} \equiv \sqrt{1 - 1/\Gamma^2}$ .

The well-known photon index  $-2/3$  for the synchrotron function (Rybicki and Lightman 1979) is obtained from  $F_q(\chi)$

in the limit of  $\chi \ll 1$ . Even for the range of  $10^{-2}\varepsilon_p - 10^{-1.5}\varepsilon_p$ , however, the functions are fitted with a photon index between  $-0.84$  and  $-0.79$ . This is seen in the low-energy slope for narrow jet opening angle of  $\theta_j = 0.1/\Gamma$  or  $1/\Gamma$  in Figure 4. For the large opening angle of  $10/\Gamma$ , the off-axis contribution slightly enhances the low-energy flux, which results in a photon index of  $\sim -1$ . This slight modification obtained numerically may be hard to be treated analytically. If the jet has angle-dependent spectrum like the model of [Lundman, Pe'er & Ryde \(2013\)](#), various photon index would be obtained.

## 6 SUMMARY

We have discussed the stochastic acceleration by turbulence in GRB jets. Since the energy source is the turbulence, mildly relativistic turbulence is required to achieve a high radiative efficiency. When the electron spectral distribution is regulated by the balance between stochastic acceleration and synchrotron cooling, the temporal evolutions of the two combinations of the phenomenological parameters,  $N_{\text{tot}}/E_0^2$  and  $BE_0^2$ , determine the final photon spectrum. If we choose an ideal parameter set, the photon spectrum can be fitted with the typical Band parameters  $\alpha \sim -1$  and  $\beta \sim -2.5$ . The off-axis contribution can soften the low-energy photon index further. The hard-to-soft evolution of photon spectrum due to the decay of the turbulence in our model may agree with the observed signatures ([Norris et al. 1986](#); [Bhat et al. 1994](#); [Ford et al. 1995](#)). The duration of the stochastic acceleration should be much shorter than the dynamical timescale for fiducial values of the magnetic field. The injection of the secondary electron–positron pairs may control the duration timescale.

The required parameter set is translated into the temporal indices for the evolutions of the diffusion coefficient, magnetic field, and total electron number. The excitation mechanism and evolution of the turbulence in GRB jets are highly uncertain. The verifications of the turbulence evolution and details of the acceleration mechanism are beyond the scope of this paper. However, the implication obtained from the recent numerical simulations of decaying MHD turbulence ([Inoue et al. 2011](#); [Zrake 2014](#); [Brandenburg, Kahniashvili & Tevzadze 2015](#)) seems encouraging for the required parameter evolutions. We can expect that future simulations of electron acceleration in turbulence, including the cases with magnetic reconnection ([Hoshino 2012](#); [Kagan, Milosavljević & Spitkovsky 2013](#); [Dahlin, Drake & Swisdak 2014](#)), reveal the excitation mechanism and initial condition of the turbulence to reproduce the GRB emissions.

## ACKNOWLEDGEMENTS

We appreciate the anonymous referee for the helpful advice. This work is partially supported by the Grant-in-Aid for Scientific Research, No. 25400227 from the MEXT of Japan.

## REFERENCES

- Abdo, A. A., et al. 2009, *Science*, 323, 1688  
 Ackermann, M., Ajello, M., Baldini, L., et al. 2012, *ApJ*, 754, 121  
 Aharonian, F. A., Atoyan, A. M., & Nahapetian, A. 1986, *A&A*, 162, L1  
 Asano, K., & Hayashida, M. 2015, *ApJL* in press, arXiv:1507.00514  
 Asano, K., & Mészáros, P. 2011, *ApJ*, 739, 103  
 Asano, K., & Mészáros, P. 2013, *JCAP*, 9, 8  
 Asano, K., & Takahara, F. 2003, *PASJ*, 55, 433  
 Asano, K., Takahara, F., Kusunose, M., Toma, K., & Kakuwa, J. 2014, *ApJ*, 780, 64  
 Asano, K., & Terasawa, T. 2009, *ApJ*, 705, 1714  
 Band, D. et al. 1993, *ApJ*, 413, 281  
 Becker, P. A., Le, T., & Dermer, C. D. 2006, *ApJ*, 647, 539  
 Bhat, P. N., Fishman, G. J., Meegan, C. A., et al. 1994, *ApJ*, 426, 604  
 Blandford, R., & Eichler, D. 1987, *PhR*, 154, 1  
 Bošnjak, Ž., Daigne, F., & Dubus, G. 2009, *A&A*, 498, 677  
 Bošnjak, Ž., & Daigne, F. 2014, *A&A*, 568, A45  
 Brandenburg, A., Kahniashvili, T., & Tevzadze, A. G. 2015, *Phys. Rev. Lett.*, 114, 075001  
 Cho, J., & Lazarian, A. 2006, *ApJ*, 638, 811  
 Dahlin, J. T., Drake, J. F., & Swisdak, M. 2014, *Phys. Plasmas*, 21, 092304  
 Derishev, E. V., Kocharovsky, V. V., & Kocharovsky, VI. V. 2001, *A&A*, 372, 1071  
 Diltz, C., & Böttcher, M. 2014, *J. High Ene. Astrop.*, 1, 63  
 Ford, L. A., Band, D. L., Matteson, J. L., et al. 1995, *ApJ*, 439, 307  
 Fritz, K. D. 1989, *A&A*, 214, 14  
 Ghisellini, G., & Celotti, A. 1999, *ApJ*, 511, L93  
 Giannios, D. 2006, *A&A*, 457, 763  
 Hoshino, M. 2012, *Phys. Rev. Lett.*, 108, 135003  
 Inoue, T., Asano, K., & Ioka, K. 2011, *ApJ*, 734, 77  
 Kagan, D., Milosavljević, M., & Spitkovsky, A. 2013, *ApJ*, 774, 41

- Kakuwa, J., Toma, K., Asano, K., Kusunose, M., & Takahara, F. 2015, MNRAS, 449, 551  
Lefa, E., Rieger, F. M., & Aharonian, F. 2011, ApJ, 740, 64  
Lundman, C., Pe'er, A., & Ryde, F. 2013, MNRAS, 428, 2430  
Lynn, J. W., Quataert, E., Chandran, B. D. G., & Parrish, I. J. 2014, ApJ, 791, 71  
Matsumoto, J., & Masada, Y. 2013, ApJ, 772, L1  
Mészáros, P., & Rees, M. J. 2000, ApJ, 530, 292  
Mészáros, P., & Rees, M. J. 2001, ApJ, 556, L37  
Mizuta, A., & Aloy, M. A. 2009, ApJ, 699, 1261  
Murase, K., Asano, K., Terasawa, T., & Mészáros, P. 2012, ApJ, 746, 164  
Nakar, E., Ando, S., & Sari, R. 2009, ApJ, 703, 675  
Narayan, R., & Kumar, P. 2009, MNRAS, 394, L117  
Norris, J. P., Share, G. H., Messina, D. C., et al. 1986, ApJ, 301, 213  
Olesen, P. 1997, Phys. Lett. B, 398, 321  
Park, B., & Petrosian, V. 1995, ApJ, 446, 699  
Pe'er, A., Mészáros, P. & Rees, M. J. 2006, ApJ, 642, 995  
Pe'er, A., & Zhang, B. 2006, ApJ, 653, 454  
Ptuskin, V. S. 1988, Soviet Astron. Lett., 14, 255  
Ramirez-Ruiz, E., Celotti, A., & Rees, M. J. 2002, MNRAS, 337, 1349  
Rybicki, G. B., & Lightman, A. P. 1979, Radiative Processes in Astrophysics (New York: Wiley-Interscience)  
Schlickeiser, R. 1984, A&A, 136, 227  
Schlickeiser, R. 1985, A&A, 143, 431  
Son, D. T. 1999, Phys. Rev. D, 59, 063008  
Stawarz, L., & Petrosian, V. 2008, ApJ, 681, 1725  
Stern, B. E., & Poutanen, J. 2004, MNRAS, 352, L35  
Vurm, I., & Poutanen, J. 2009, ApJ, 698, 293  
Wang, X.-Y., Li, Z., Dai, Z.-G., & Mészáros, P. 2009, ApJ, 698, 98  
Yan, H., & Lazarian, A. 2008, ApJ, 673, 942  
Zirakashvili, V. N., & Aharonian, F. A. 2007, A&A, 465, 695  
Zhang, B., Liang, E., Kim, L. P., et al. 2007, ApJ, 655, 989  
Zhang, W., Woosley, S. E., & MacFadyen, A. I. 2003, ApJ, 586, 356  
Zhao, X., Li, Z., Liu, X., Zhang, B.-B., Bai, J., & Mészáros, P. 2014, ApJ, 780, 12  
Zrake, J. 2014, ApJ, 794, L26

This paper has been typeset from a  $\text{\TeX}/\text{\LaTeX}$  file prepared by the author.